

VFP: Variational Flow-Matching Policy for Multi-Modal Robot Manipulation

Xuanran Zhai¹, Ce Hao^{*1}

¹ National University of Singapore

* Corresponding to cehao@u.nus.edu

Abstract

Flow-matching-based policies have recently emerged as a promising approach for learning-based robot manipulation, offering significant acceleration in action sampling compared to diffusion-based policies. However, conventional flow-matching methods struggle with multi-modality, often collapsing to averaged or ambiguous behaviors in complex manipulation tasks. To address this, we propose the Variational Flow-Matching Policy (VFP), which introduces a variational latent prior for mode-aware action generation and effectively captures both task-level and trajectory-level multi-modality. VFP further incorporates Kantorovich Optimal Transport (KOT) for distribution-level alignment and utilizes a Mixture-of-Experts (MoE) decoder for mode specialization and efficient inference. We comprehensively evaluate VFP on 41 tasks across four benchmark environments, demonstrating its effectiveness and sampling efficiency in both task and path multi-modality settings. Results show that VFP achieves a 49% relative improvement in task success rate over standard flow-based baselines, while maintaining fast inference and compact model size. More details are available on our project page: <https://sites.google.com/view/varfp/>

1 Introduction

Learning-based methods have driven major advances in robot manipulation, enabling robots to generalize across a wide range of tasks from expert demonstrations (Wang et al. 2023; Handa et al. 2019; Shridhar, Manuelli, and Fox 2022). Among these approaches, diffusion-based policies have shown impressive results in multi-modal imitation learning by leveraging stochastic denoising to capture the diverse action distributions present in real-world tasks (Chi et al. 2023; Ze et al. 2024; Wang et al. 2024a; Lu et al. 2024; Wang et al. 2024b). Yet, the slow, iterative sampling process of diffusion models limits their practicality for real-time control. To address this, flow-matching (FM) policies (Rouxel et al. 2024; Zhang et al. 2024; Zhang and Gienger 2025; Braun et al. 2024) have emerged as a promising alternative, employing probabilistic flow-based ODEs for much faster action generation—requiring only a single ODE integration step. In practice, flow-matching policies can reduce sampling time to just 20% of that needed by diffusion models, making them highly attractive for time-sensitive robot manipulation tasks.

However, flow-matching policies struggle to capture the inherent multi-modal distributions found in robot manipu-

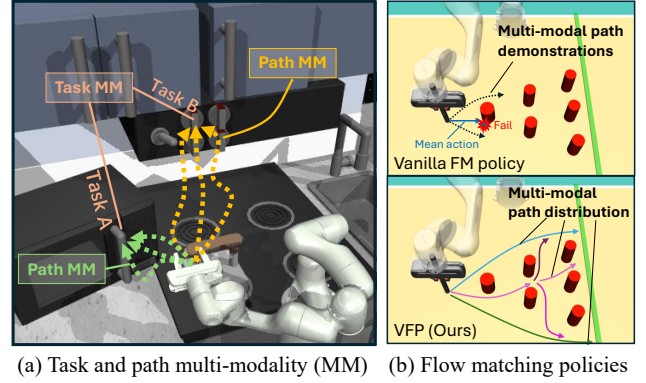


Figure 1: **(a)** In Franka kitchen environment, the robot finishes multiple tasks and each task has different paths, which requires the policy to capture the task and path multi-modality (MM). **(b)** In the avoiding task, the vanilla flow-matching (FM) policy learns the mean action over all demonstrations, while our variational flow-matching policy (VFP) successfully follows the MM path distribution.

lation tasks. As illustrated in Fig. 1 (a), a robot operating in a kitchen environment faces both task-level and path-level multi-modality, where it must not only accomplish different objectives but may also follow various demonstrated paths to complete each task. Flow matching, formulated as an ODE-based generative model, is fundamentally limited in representing such multi-modal behavior with neural networks (Samaddar et al. 2025; Chen et al. 2025; Guo and Schwing 2025). For example, as shown in Fig. 1 (b), when a robot must plan collision-free paths, the flow-matching policy often averages over all demonstrated options, resulting in actions that do not correspond to any valid path. This averaging effect leads to significant failures in imitation learning for manipulation tasks where representing diverse and distinct behaviors is essential.

To address this limitation, we propose the *Variational Flow-Matching Policy* (VFP) for fast and expressive multi-modal policy generation in robot manipulation (Fig. 1 (b)). The key idea of VFP is to use a variational latent prior to capture the inherent multi-modality in expert demonstrations, while employing a flow-matching model as a conditional decoder that generates actions specific to each mode. This variational formulation shifts the burden of mode identification

to the latent prior, effectively avoiding the averaging effect of standard flow matching and enabling the policy to model diverse behaviors. To further align the learned action distribution with the multi-modal expert data, we introduce Kantorovich Optimal Transport (K-OT) (Peyré and Cuturi 2020; Cuturi 2013; Villani and Society 2003) as a distribution-level regularization, which directly matches the predicted and expert action distributions for each state and promotes clear mode separation. Additionally, we implement the flow decoder as a Mixture-of-Experts (MoE) model (Jordan and Jacobs 1993; Jacobs et al. 1991), allowing each expert to focus on a distinct behavioral mode and improving both multi-modality representation and sampling efficiency. Through the integration of variational inference, K-OT distribution matching, and MoE expert specialization, VFP achieves robust and real-time multi-modal imitation learning in complex robot manipulation tasks.

We validate the effectiveness and computational efficiency of VFP in both task and path multi-modality environments. For task multi-modality, we evaluate on the Franka Kitchen benchmark (Gupta et al. 2019), where multiple tasks coexist and can be completed in arbitrary order. In this setting, FlowPolicy (Zhang et al. 2024) exhibits unstable, indecisive behaviors due to mode averaging, while VFP clearly distinguishes and executes distinct task modes, achieving an 11.5% improvement in task success rate. For path multi-modality, we test on D3IL (Jia et al. 2024) as well as the large-scale Adroit (Rajeswaran et al. 2018) and Meta-World (Yu et al. 2021) environments, which collectively cover 30 tasks with diverse demonstrated trajectories. Across these benchmarks, VFP outperforms FlowPolicy by 61.7% in average success rate, while maintaining comparable inference time and model size. In addition, our results show that VFP effectively balances multi-modal policy representation with computational efficiency, consistently achieving high performance in complex tasks without sacrificing the fast inference advantage of flow-matching models.

In summary, our main contributions are:

- We propose Variational Flow-Matching Policy (VFP), a new imitation learning framework that uses a variational latent prior for mode identification, effectively overcoming the averaging problem in flow-matching models.
- We introduce Kantorovich Optimal Transport (K-OT) for explicit distribution alignment and employ a Mixture-of-Experts (MoE) decoder to enhance multi-modal expressiveness and computational efficiency.
- We extensively validate VFP on diverse benchmarks, demonstrating an average improvement of 49% in success rate across all tasks and 94% on highly multi-modal benchmarks, while maintaining fast inference.

2 Related Works

Flow Matching. Flow Matching (FM) (Lipman et al. 2023; Albergo and Vanden-Eijnden 2023; Liu, Gong, and Liu 2022) is a class of generative modeling methods that learn continuous-time vector fields to transport samples from a source distribution to a target distribution. The conceptual roots of FM can be traced back to Normalizing Flows (Kobyzev, Prince, and Brubaker 2021; Papamakarios

et al. 2021; Huang, Dinh, and Courville 2020) and Neural ODEs (Chen et al. 2019), where invertible transformations or flow-based dynamics are used to model complex distributions. In contrast to traditional Normalizing Flows, FM directly learns a velocity field without requiring invertibility, enabling more flexible modeling. Recent advances in Flow Matching include several instantiations of the framework, such as Rectified Flow (Liu, Gong, and Liu 2022), Consistency Models (Yang et al. 2024), and Flow Matching for Score-based Modeling (Lipman et al. 2023), which propose different formulations of matching objectives. These methods have shown competitive generation quality.

Multi-modality in Robot Manipulation. Multi-modality (MM), a prevalent characteristic in robotic manipulation tasks, primarily consists of task and path multi-modality. Task MM arises in environments with multiple valid task objectives (e.g., Franka Kitchen), whereas path MM is even more common, as there are typically multiple feasible trajectories to achieve the same goal. For example, an object can be pushed from one location to another along different paths, all of which are functionally correct. To model such diversity, prior works have explored mixture models like MDNs (Bishop 1994), and latent-variable methods such as conditional VAEs (Hausman et al. 2017). More recently, diffusion-based approaches (Chi et al. 2023; Ze et al. 2024) have shown success in capturing multi-modal distributions through denoising-based generation. However, while flow matching holds great potential for imitation learning due to its fast inference speed, apart from some recent works (Zhang and Gienger 2025) that rely on large pretrained vision-language models, to the best of our knowledge, no existing flow-based approach has addressed multi-modal behavior modeling in imitation learning.

3 Preliminary

Problem Formulation. We consider robot manipulation tasks \mathcal{T} , where the goal is to train a policy $p_\theta(a|s)$ parameterized by θ via imitation learning. States $s \in \mathcal{S}$ and actions $a \in \mathcal{A}$ are observed and executed in a manipulation environment. Given a dataset of expert demonstrations $\mathcal{D} = \{(s_i, a_i)\}$, the policy is trained by maximizing the conditional log-likelihood $\mathbb{E}_{(s,a) \sim \mathcal{D}} [\log p(a|s)]$.

Flow Matching. Flow matching formulates generative modeling as learning a velocity field that deterministically transports samples from a source distribution to a target distribution along a continuous trajectory. In the context of policy learning for robot manipulation, this corresponds to learning a time-dependent velocity field $v_\theta(a, t, s)$ that maps an initial action $a_0 \sim p_0(a_0|s)$ to a target action $a_1 \sim p_1(a_1|s)$.

At inference time, a sample a_0 is drawn from the source distribution $p_0(a_0|s)$ and treated as the initial condition for an ordinary differential equation (ODE). This ODE is solved by integrating the velocity field $v_\theta(a_t, t, s)$ forward from $t = 0$ to $t = 1$, with a_t following a trajectory (e.g., linear interpolation: $a_t = (1-t)a_0 + ta_1$ in rectified flow matching (Liu, Gong, and Liu 2022)) between a_0 and a_1 . The likelihood of a data point a_1 under this model can be as-

sessed using the instantaneous change-of-variables formula:

$$\log p_1(a_1) = \log p_0(a_0) + \int_1^0 \operatorname{div} v_\theta(a_t, t, s) dt, \quad (1)$$

where div denotes the divergence operator. During training, pairs of samples (a_0, a_1) and a time $t \in [0, 1]$ are drawn, and the interpolated location $a_t = (1 - t)a_0 + ta_1$ is computed. The ground-truth velocity at this point is $v(a_0, a_1, t) = a_1 - a_0$, which is used as the target for the model’s parametric velocity field. The flow matching objective is to minimize the mean squared error between the learned and ground-truth velocities:

$$\mathcal{L}_{\text{FM}} = \mathbb{E}_{s, a_0, a_1, t} [\|v_\theta(a_t, t, s) - (a_1 - a_0)\|^2]. \quad (2)$$

This approach allows flow matching to flexibly model complex action distributions by learning deterministic trajectories between source and target actions for any given state s . The method provides both efficient sampling—via ODE integration—and principled likelihood evaluation—via the change-of-variables formula—making it well-suited for high-dimensional generative modeling in robotics and imitation learning.

Velocity Ambiguity of Flow Matching. While flow-based models offer efficient and deterministic generative modeling, they are fundamentally challenged by *velocity ambiguity* in multi-modal settings. In many real-world robotic tasks, it is common for multiple distinct action trajectories to pass through the same interpolated point (a_t, t, s) , typically when $t = 0$, each associated with a different underlying velocity $v^* = a_1 - a_0$. In these cases, the flow matching model must assign a unique velocity vector to every (a_t, t, s) , even though several valid options exist in the data. The standard flow matching objective, $\mathcal{L}_{\text{FM}} = \sum_{i=1}^n \|v_\theta(a_t, t, s) - v(a_0^i, a_1^i, t, s)\|_2^2$, requires the model to regress to a single “best” velocity at each point. Consequently, the optimal solution is for the model to predict the average of all feasible ground-truth velocities that pass through the point:

$$v_\theta^*(a_t, t, s) = \mathbb{E}_i [v(a_0^i, a_1^i, t, s) \mid a_t, t, s]. \quad (3)$$

This leads to *mode mixing* (*averaging effect*): the predicted velocity may not correspond to any actual expert trajectory, particularly when the data is highly multi-modal. As a result, standard flow matching tends to blur or average over distinct modes, and cannot faithfully represent the true diversity of expert behaviors—highlighting the need for explicit mechanisms to handle multi-modality.

4 Method

In this section, we present the *Variational Flow Matching Policy* (VFP) framework. VFP employs a variational approach to infer a latent code z , which determines the mode selection within the downstream flow matching model (Sec. 4.1). To prevent averaging effect, VFP introduces the static Kantorovich-Optimal Transport (K-OT) regularization, which promotes multi-modal distribution matching in both latent and action distributions throughout the flow matching process (Sec. 4.2). Furthermore, VFP enhances

multi-modal expressiveness by incorporating a mixture-of-experts (MoE) structured flow matching decoder, demonstrating a principled integration of variational inference and MoE for robust policy learning (Sec. 4.3). An overview of our method is in Fig. 2.

4.1 Variational Flow Matching Structure

In many real-world robot manipulation tasks, the optimal policy $p(a|s)$ is inherently *multi-modal* (MM): given a state s , there may exist several distinct, equally valid action choices a . Standard learning objectives, such as maximum likelihood or mean-squared error, are insufficient for such settings—they encourage the model to average across modes, producing unrealistic or ambiguous predictions.

Multi-Modality Ambiguity Estimation. To rigorously measure the magnitude of multi-modality (or ambiguity), we adopt an *ambiguity metric* based on the conditional variance of ground-truth velocities in flow matching. For each state s and interpolated time t , consider trajectories that pass through a common intermediate action $a_t = (1 - t)a_0 + ta_1$, with a_0 and a_1 sampled from the data. The oracle velocity for each pair is defined as $v^* = a_1 - a_0$. The per-point ambiguity at (a_t, t, s) is then quantified by the conditional variance:

$$\operatorname{Var}[v^* \mid a_t, t, s] = \mathbb{E}_{(a_0, a_1) \mid a_t, t, s} [\|v^* - \mu_v\|_2^2], \quad (4)$$

where $\mu_v = \mathbb{E}_{(a_0, a_1) \mid a_t, t, s} [v^*]$.

This measures the spread of all possible velocities for trajectories passing through the same (a_t, t, s) . To summarize the overall ambiguity in the data, we define the global ambiguity score by averaging over the data distribution:

$$\mathcal{A}_{\text{FM}} = \mathbb{E}_{(a_0, a_1, t, s)} [\operatorname{Var}[v^* \mid a_t, t, s]]. \quad (5)$$

A high value of \mathcal{A}_{FM} indicates substantial multi-modality in the expert demonstrations. However, standard flow matching models are fundamentally limited in handling this ambiguity. When multiple distinct trajectories intersect at the same (a_t, t, s) with different velocities, the model must choose a single velocity for each point. Even with infinite data and perfect optimization, the best the model can do is predict the mean velocity μ_v at each point. Thus, the irreducible loss—i.e., the minimum achievable FM loss—is exactly the ambiguity score \mathcal{A}_{FM} . This “crossing term” is intrinsic: *no deterministic flow matching model can reduce the ambiguity below this floor without an additional mechanism for mode separation*. For a detailed proof, see Appendix A.2.

Variational Flow Matching Policy (VFP) Formulation.

To address the irreducible ambiguity in standard flow matching, we propose a *Variational Flow Matching Policy* (VFP), which leverages variational inference to capture and disentangle multi-modal structure in the data. As illustrated in Fig. 2 (B), the key idea is to introduce a latent variable z that indexes different modes of the action distribution for each state s . The overall policy becomes:

$$p_{\theta, \psi}(a \mid s) = \int p_\theta(a \mid z, s) p_\psi(z \mid s) dz, \quad (6)$$

where $p_\psi(z \mid s)$ is a learned variational encoder (the “prior”), and $p_\theta(a \mid z, s)$ is a flow-based decoder conditioned on both z and s .

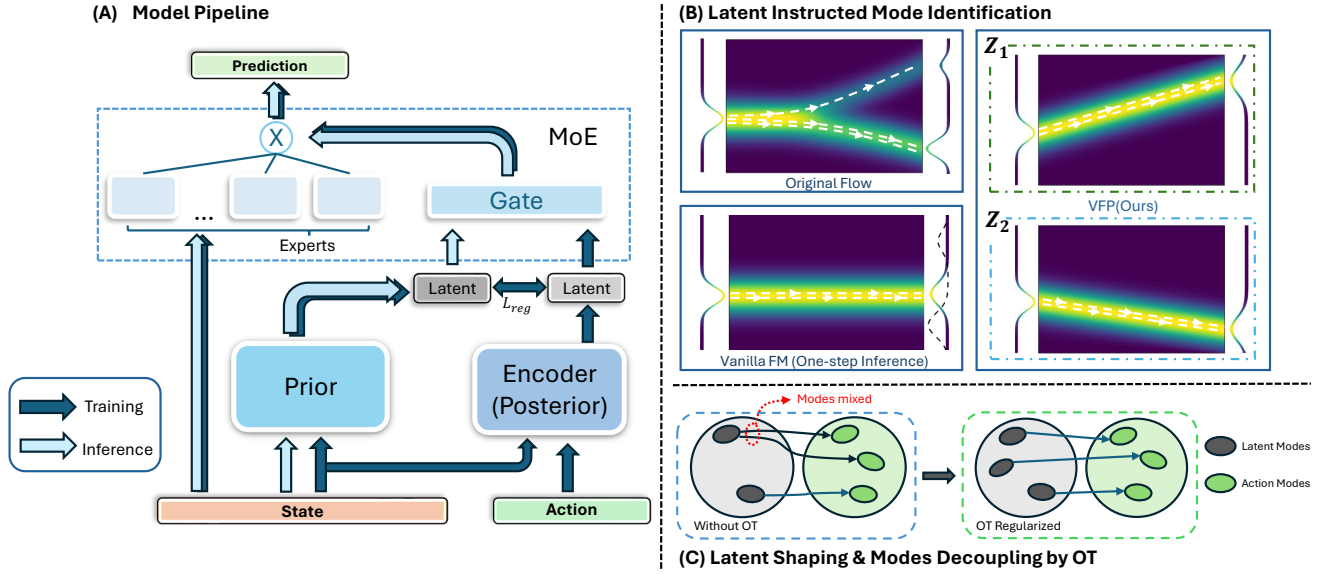


Figure 2: **Overview of Variational Flow Policy (VFP).** (A) **Model Pipeline:** The model consists of a latent-conditioned Mixture-of-Experts (MoE) flow matching network. A prior network generates latent variables from input states, which guide the MoE decoder to predict actions efficiently. During training, a posterior encoder is used for variational learning. (B) **Latent-Instructed Mode Identification:** Visualization of how VFP enables mode-specific behavior. Compared to the collapsed predictions of vanilla flow matching, our model captures distinct modes conditioned on latent variables. (C) **Latent Shaping and Mode Decoupling via OT:** Optimal Transport regularization improves mode separation in the latent space, aligning latent modes with distinct action modes.

The flow matching decoder in VFP is constructed similarly to standard FM, but is now conditioned on the latent z . For each training example, given (s, a_0, a_1, t) and sampled z , we define the interpolated action $a_t = (1-t)a_0 + ta_1$, and train a velocity field $v_\theta(a_t, t, s, z)$ to match the ground-truth displacement $v^* = a_1 - a_0$:

$$\mathcal{L}_{\text{FM}} = \mathbb{E}_{s, a_0, a_1, t, z} [\|v_\theta(a_t, t, s, z) - (a_1 - a_0)\|^2]. \quad (7)$$

For training, we adopt a variational lower bound (ELBO) objective, introducing a recognition network $q_\phi(z | a, s)$ to approximate the intractable posterior over z . The overall VFP objective is:

$$\mathcal{L}_{\text{VFP}} = \mathbb{E}_{(s, a) \sim \mathcal{D}, z \sim q_\phi(z | a, s)} [-\mathcal{L}_{\text{FM}}(a, s, z) - D_{\text{KL}}(q_\phi(z | a, s) \| p_\psi(z | s))]. \quad (8)$$

This objective encourages the encoder $p_\psi(z | s)$ to capture the multi-modal structure of $p(a | s)$, while the decoder $p_\theta(a | z, s)$ learns to model mode-specific, nearly deterministic action flows. By maximizing the ELBO in the context of flow matching, VFP both explains the diversity in the data and regularizes the latent space for generalization.

Multi-Modality Ambiguity Decomposition. The key theoretical advantage of VFP is that it enables the model to attribute the multi-modality (ambiguity) in the data to the latent variable z , thereby simplifying the flow decoder. This can be formalized by decomposing the total ambiguity using the law of total variance. For a fixed (a_t, t, s) , the conditional variance of oracle velocities can be written as:

$$\text{Var}[v^* | a_t, t, s] = \mathbb{E}_{z | a_t, t, s} [\text{Var}[v^* | a_t, t, s, z]] + \text{Var}_{z | a_t, t, s} (\mathbb{E}[v^* | a_t, t, s, z]). \quad (9)$$

Here, the first term is the *residual ambiguity* remaining in the decoder after conditioning on z , and the second term quantifies the ambiguity explained by the latent variable. Averaged over the dataset, the global ambiguity score decomposes as:

$$\mathcal{A}_{\text{FM}} = \mathcal{A}_{\text{VFP}} + \mathbb{E}_{(a_t, t, s)} [\text{Var}_{z | a_t, t, s} (\mu_v | z)], \quad (10)$$

where $\mathcal{A}_{\text{VFP}} = \mathbb{E}_{(a_0, a_1, t, s)} [\text{Var}[v^* | a_t, t, s, z]]$.

The second term is always non-negative, yielding the following inequality $\mathcal{A}_{\text{VFP}} \leq \mathcal{A}_{\text{FM}}$. This proves that variational conditioning strictly reduces or matches the ambiguity present in standard flow matching. For a detailed proof, see Appendix A.3.

For VFP to be maximally effective, the encoder $p(z | s)$ should capture as much of the data’s multi-modality as possible—i.e., assign distinct z values to different modes. In the ideal case, where each z uniquely identifies a mode, the residual decoder ambiguity \mathcal{A}_{VFP} is minimized, and $p_\theta(a | z, s)$ becomes nearly unimodal. Thus, VFP enables the policy to represent highly multi-modal action distributions without forcing the decoder to average over modes, fundamentally overcoming the limitations of standard flow matching in complex, ambiguous settings.

4.2 Kantorovich-OT for Distribution Matching

In multi-modal imitation learning, the central challenge is to match the *entire* conditional action distribution $p(a | s)$ induced by the expert, not just individual demonstration pairs. For any given state s , the expert policy $p_{\text{expert}}(a | s)$ may assign probability mass to multiple diverse actions a , reflecting the inherent ambiguity and richness of real-world decision-making. Conventional flow matching and sample-based imitation approaches focus on aligning isolated samples or tra-

jectories, i.e., matching (s, a) pairs. However, such point-wise objectives are fundamentally limited: they often induce mode averaging, resulting in learned policies $p_\theta(a | s)$ that underrepresent the true diversity of expert behaviors. To faithfully imitate expert demonstrations in multi-modal settings, it is essential to align distributions at the population level—ensuring that $p_\theta(a | s)$ covers all modes present in $p_{\text{expert}}(a | s)$ for each state s .

Kantorovich-Optimal Transport (K-OT) Formulation.

The K-OT framework provides a principled approach to aligning probability distributions by minimizing the cost of transporting probability mass from one distribution to another. In the setting of multi-modal imitation learning, for each state s , we consider two discrete distributions: the predicted action distribution $p_\theta(a | s) = \sum_i u_i \delta_{a_i}$ (where a_i are samples from the policy) and the empirical expert action distribution $p_{\text{expert}}(a | s) = \sum_j v_j \delta_{a'_j}$ (where a'_j are expert demonstrations). Here, u_i and v_j are normalized weights summing to one, and δ_a denotes a Dirac delta at a .

The K-OT distance between $p_\theta(a | s)$ and $p_{\text{expert}}(a | s)$ is defined as the minimum total transport cost under a ground cost $\mathcal{C}(a, a')$:

$$\text{OT}(p_\theta, p_{\text{expert}}) = \min_{\gamma \in \Pi(u, v)} \sum_{i, j} \gamma_{i, j} \mathcal{C}(a_i, a'_j), \quad (11)$$

where $\gamma \in \Pi(u, v)$ denotes the set of all valid couplings (transport plans) between the two distributions with marginals u and v . Typically, the ground cost is chosen as the squared Euclidean distance $\mathcal{C}(a, a') = \|a - a'\|^2$. This formulation encourages each predicted action to be matched with a similar expert action, while the optimal coupling γ ensures the entire distribution—across all modes—is faithfully aligned. In practice, since states are continuous, we define the OT cost as $\|a - a'\|^2 + \lambda \|s - s'\|^2$ to enable soft cross-condition matching without requiring exact state alignment. We adopt Sinkhorn optimal transport to efficiently compute a differentiable form of this regularization.

K-OT Regularization. To promote faithful multi-modal imitation, we introduce Kantorovich-Optimal Transport (K-OT) as a regularization term in the training objective. For each mini-batch, we sample sets of actions from the policy $p_\theta(a | s)$ and the expert demonstrations $p_{\text{expert}}(a | s)$ for each state s . The K-OT distance between these sets is then computed and used to regularize the learning process:

$$\mathcal{L}_{\text{total}} = \mathcal{L}_{\text{VFP}} + \alpha \mathbb{E}_s [\text{OT}(p_\theta(a | s), p_{\text{expert}}(a | s))], \quad (12)$$

where α is a weighting coefficient controlling the influence of K-OT regularization. This approach ensures that, beyond trajectory-level imitation via variational flow matching, the model is explicitly encouraged to align the entire predicted action distribution with the expert’s for each state. Therefore, as depicted in Fig. 2 (C), K-OT regularization helps the policy cover all demonstrated modes, mitigates averaging effect, and produces more diverse and expressive behaviors that better reflect the richness of expert demonstrations.

4.3 VFP Implementation

To further enhance the model’s capacity for multi-modality and accelerate both training and inference, as shown in

Fig. 2 (A), we implement the policy decoder as a **Mixture-of-Experts (MoE)**. The MoE structure enables each expert to specialize in a particular behavioral mode, while the gating network efficiently selects and combines expert predictions. This architecture not only improves expressiveness for complex, multi-modal action distributions, but also allows for parallelized computation and scalable learning.

In our VFP framework, multi-modality is captured in the latent variable z , which is sampled from a diffusion-based prior $p_\psi(z | s)$. The decoder is a Mixture-of-Experts (MoE) flow model, where the velocity field consists of K flow matching experts. Each expert $v_{\theta, i}(a_t, t, s)$ models a distinct behavioral mode, and a gating network maps z to a set of coefficients $\{g_i(z)\}_{i=1}^K$ satisfying $\sum_{i=1}^K g_i(z) = 1$. Therefore, during training, we use a decoupled loss formulation where each expert is trained independently, and the total loss is computed as a gating-weighted sum:

$$\mathcal{L}_{\text{VFP}} = \mathcal{L}_{\text{MoE}} = \sum_{i=1}^K g_i(z) \cdot \|v_{\theta, i}(a_t, t, s) - v\|^2. \quad (13)$$

This encourages expert specialization, where each expert independently fit a mode. Accordingly, during inference, we select the expert with the highest gating weight, i.e., $i^* = \arg \max_i g_i(z)$, and generate actions using only v_{θ, i^*} .

To summarize, the overall VFP framework leverages a diffusion-based latent prior and a Mixture-of-Experts flow decoder to enable robust and expressive multi-modal policy learning. The full training and sampling procedures are detailed in Appendix B.1 and B.2. By integrating variational inference, K-OT regularization, and expert specialization, VFP achieves efficient distribution-level alignment and adaptive, diverse robot behavior in complex manipulation tasks.

5 Experiments

We empirically evaluate the proposed VFP framework on a suite of challenging, multi-modal robot manipulation tasks. Our experiments are designed to answer the following core questions:

- **Effectiveness:** Does VFP improve manipulation performance in multi-modal settings compared to baseline methods?
- **Efficiency:** Can VFP maintain the fast inference advantage of traditional flow-matching models? Does it require more computational resources?
- **Ablation:** How important are K-OT regularization and the Mixture-of-Experts (MoE) flow decoder for achieving state-of-the-art results?

The remainder of this section describes our experimental setup, baselines, evaluation protocols, and results.

5.1 Experiment Setting

Environments. We evaluate VFP in two categories of multi-modal robot manipulation environments: task and path multi-modality. For task multi-modality, where policies should commit to a specific objective instead of mixing multiple tasks, we use the Franka Kitchen environment (Gupta

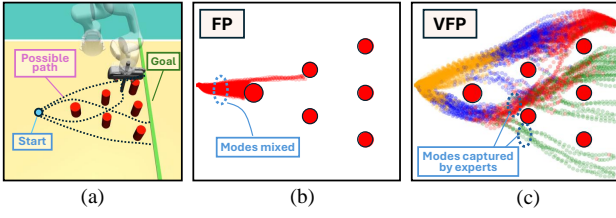


Figure 3: The Avoiding task and behaviors of policies. (a): The environment of avoiding. (b): Behavior of FlowPolicy (red trajectories). (c): Behavior of VFP (ours). Movements made by different experts are in different colors.

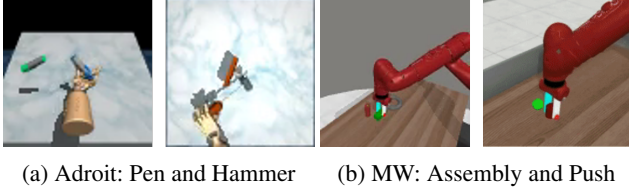


Figure 4: Tasks in (a) Adroit and (b) Meta-World.

et al. 2019) (shown in Fig. 1 (a)), which requires the robot to complete any subset of seven distinct kitchen tasks in arbitrary order, and the block pushing scenario in D3IL (Jia et al. 2024), where two tasks must be solved in any sequence. For path multi-modality, where the policy must distinguish between different valid trajectories rather than averaging them, we consider the D3IL obstacle avoidance task (shown in Fig. 3) as a clear example, since the robot can reach its goal by avoiding obstacles via multiple distinct paths. To further validate our approach, we also evaluate on two large-scale environments, Adroit (Rajeswaran et al. 2018) and Meta-World (Yu et al. 2021) (shown in Fig 4), both featuring a wide range of tasks where each task admits multiple feasible paths due to the diversity of human demonstrations.

Baselines and Evaluation Metrics. We compare VFP to state-of-the-art diffusion- and flow-based imitation learning methods, including Diffusion Policy (DP) (Chi et al. 2023), 3D Diffusion Policy (DP3) (Ze et al. 2024), and FlowPolicy (FP) (Zhang et al. 2024). These baselines are chosen for their strong performance on multi-modal robot manipulation benchmarks. To evaluate effectiveness, we report task rewards (success rates) averaged over multiple random seeds and episodes. For efficiency, we measure inference time (IT), the number of function evaluations (NFE), and computational resource usage, quantified by the number of active NN parameters used during policy inference.

5.2 Experiment Results

VFP achieves task multi-modality by latent mode selection. We evaluate our method on the Franka Kitchen benchmark, which requires the agent to select and complete multiple tasks within a single environment. In the experiments, we observe that FlowPolicy often oscillates between tasks—such as switching repeatedly among the three light switches in the turn-on-light task—and this indecision also leads to frequent failures in handle grasping tasks. In contrast, our VFP leverages the latent prior to effectively distinguish between task modes, enabling the flow-matching

Methods	D3IL (%)				Kitchen
	Avoiding	Sorting-4	Pushing		
DP	0.89±0.01	0.30±0.06	0.92±0.03		3.99
Flowpolicy	0.02±0.01	0.14±0.01	0.67±0.02		3.64
VFP (ours)	0.91±0.01	0.45±0.01	0.94±0.02		4.06

Table 1: Success Rate/Reward on D3IL and Franka Kitchen

decoder to generate consistent and smooth trajectories for each selected task. As a result, VFP increases the average rewards in Franka Kitchen by 11.5% (Tab. 1), compared to FlowPolicy. Also, in the Pushing task from D3IL, our success increases by 40.2%.

VFP captures path multi-modality by disentangling trajectory modes. We evaluate path-level multi-modality on the D3IL benchmark, where each task permits multiple valid trajectories to reach the goal. As shown in Tab. 1, VFP significantly outperforms baseline methods across all three tasks. As shown in figure 3, FlowPolicy frequently exhibits averaging behavior, causing the agent to move directly into obstacles instead of selecting a valid path around them. In contrast, VFP effectively captures the multi-modal structure of the demonstrations, enabling the agent to reliably choose distinct trajectories. It’s also shown in figure 3 that our model produces diverse behaviors in rollouts, with different experts specializing in different trajectory modes.

We also evaluate VFP on the large-scale Adroit and Meta-World manipulation environments. While multi-modality in these benchmarks is generally less pronounced than in D3IL, some complex tasks—such as swinging a hammer or rotating a pen—feature various possible trajectories and thus introduce path-level multi-modality. Overall, VFP improves average performance across all tasks by about 4% compared to FlowPolicy, yielding comparable results. However, for more challenging tasks that require greater precision and control, VFP provides more substantial gains. For example, in the Adroit “Pen” task, where the agent must use dexterous hand movements to rotate a pen, FlowPolicy often falls back on crude wrist oscillations instead of the fine finger manipulations needed for successful rotation. This is likely due to mode mixing, where distinct rotation strategies become entangled in the model’s output distribution, preventing the policy from committing to an effective trajectory. In contrast, VFP avoids this issue and increases the average success rate by 15% on the “Pen” task. Similarly, for “Very Hard” tasks in Meta-World, VFP achieves a 10% improvement over FlowPolicy.

Model Efficiency. We evaluate the average inference time and model size on D3IL, Adroit, and Meta-World. As shown in Table 3, our method incurs only a 5.6% increase in inference time compared to FlowPolicy, while remaining 4.6× faster than diffusion-based models. The active model size remains comparable overall, and is even 4.9% smaller on Adroit and Meta-World. Although VFP incorporates additional components and achieves substantially improved performance, it still maintains high computational efficiency. This is primarily due to the Mixture-of-Experts (MoE) decoder, which decomposes the overall task into smaller sub-problems handled by individual experts. Each expert oper-

Methods	NFE	Adroit (%)			Meta-World (%)				Average (%)
		Hammer	Door	Pen	Easy(21)	Medium(4)	Hard(4)	Very Hard(5)	
DP	10	16±10	34±11	13±2	50.7±6.1	11.0±2.5	5.25±2.5	22.0±5.0	35.2±5.3
DP3	10	100±0	56±5	46±10	87.3±2.2	44.5±8.7	32.7±7.7	39.4±9.0	68.7±4.7
FlowPolicy	1	100±0	58±5	53±12	90.2±2.8	47.5±7.7	37.2±7.2	36.6±7.6	70.0±4.7
VFP (Ours)	1	99±1	64±3	61±8	91.5±1.2	48.4±8.1	37.8±8.2	40.5±6.7	72.8±3.7
VFP w/o K-OT	1	96±3	61±6	54±13	90.8±1.7	48.2±8.8	36.5±9.1	36.2±7.2	71.3±4.4
VFP w/o MoE	1	94±2	57±6	50±11	88.2±4.8	46.6±9.2	35.5±5.2	35.2±4.6	69.1±5.4

Table 2: Comparison of success rates (%) \uparrow on Adroit and Meta-World tasks between state-of-the-art diffusion-based models—Diffusion Policy (Chi et al. 2023) and 3D Diffusion Policy (Ze et al. 2024)—and the flow-based model FlowPolicy (Zhang et al. 2024).

Methods	Inference time (ms) \downarrow				Active params (M) \downarrow	
	D3IL	Adroit	Metaworld	Avg.	D3IL	Adroit/MW
DP	56.2	100.3	106.5	87.7	0.59	255.1
DP3	—	145.9	145.6	—	—	255.2
FP	13.1	20.1	19.9	17.7	0.59	255.7
VFP	14.3	21.5	20.3	18.7	0.60	243.3

Table 3: Comparison on inference time and model size. “—” indicates that DP3 is not applicable to D3IL.

ates with a shallower network, thereby reducing the per-expert computational cost and keeping the overall inference overhead low.

5.3 Ablation Studies

In our ablation studies, we aim to demonstrate how VFP benefits from the OT regularization and the MoE-structured decoder in enhancing its ability to model multi-modal distributions. To this end, we primarily conduct ablation studies on D3IL and Franka Kitchen, two benchmarks that exhibit rich multi-modality and serve as suitable environments for evaluating this capability. Additionally, the ablated variants, VFP w/o K-OT and VFP w/o MoE, are also evaluated on Adroit and Meta-World to assess their generalization in broader settings.

K-OT Regularization. To investigate the effect of OT regularization, we conduct ablation studies by varying the weight of the OT loss. As reported in Tab. 2, in environments with less pronounced multi-modality (Adroit and Meta-World), OT regularization yields a modest improvement of around 2%. In contrast, as shown in Fig 5, in highly multi-modal benchmarks such as D3IL and Franka Kitchen, properly tuning the OT weight leads to performance gains of 44% and 36%, respectively, compared to models trained without OT. Moreover, the standard deviation of success rate (or reward) across different seeds decreases by approximately 27% on D3IL and 18% on Meta-World, indicating improved training stability and more consistent multi-modal behavior. These results highlight that OT regularization is particularly beneficial in multi-modal environments, enhancing both overall performance and the robustness of the learning process.

MoE Decoder. To evaluate the importance of the MoE structure, we conduct experiments using a variant where the entire MoE decoder is replaced by a single monolithic neural network, directly conditioned on the latent variable and

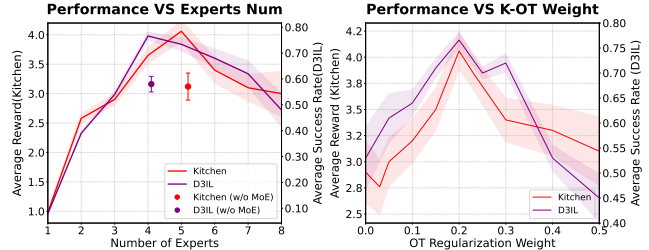


Figure 5: Ablation studies. **Left:** Performance under varying numbers of experts in the MoE decoder. Circle markers denote single-model variants without MoE, placed at x-axis positions indicating the number of experts with roughly equivalent total parameter count. **Right:** Performance under different OT regularization weights.

scaled to have a similar total number of parameters as the original MoE-based model. As shown in Tab. 2 and Fig. 5, while the MoE decoder yields a moderate average improvement of approximately 5.3% on Adroit and Meta-World, it leads to significantly larger gains on D3IL and Franka Kitchen—around 26% and 32%, respectively. These results demonstrate that, under similar model capacity, the MoE structure substantially enhances the ability to model multi-modal distributions. Additionally, to provide practical guidance on selecting the number of experts, we conduct further ablation studies. As shown in Fig. 5, increasing the number of experts initially improves performance; however, an excessively large number leads to degraded performance and training instability, likely due to the limited capacity of the gating network to effectively assign expert responsibilities.

6 Conclusion

We propose Variational Flow Policy (VFP), a method designed to effectively address multi-modality in flow-based imitation learning for robot manipulation. By leveraging a variational latent prior, Kantorovich Optimal Transport regularization, and a Mixture-of-Experts (MoE) decoder, VFP enhances both multi-modal representation and computational efficiency. Experiments on task-level and path-level multi-modality benchmarks demonstrate that VFP achieves substantial gains in task success rate while maintaining fast inference. Ablation studies further confirm the effectiveness of both K-OT regularization and the MoE decoder as key components of our framework.

References

- Albergo, M. S.; and Vanden-Eijnden, E. 2023. Building Normalizing Flows with Stochastic Interpolants. *arXiv:2209.15571*.
- Bishop, C. M. 1994. Mixture density networks.
- Braun, M.; Jaquier, N.; Roza, L.; and Asfour, T. 2024. Riemannian Flow Matching Policy for Robot Motion Learning. *arXiv:2403.10672*.
- Chen, H.; Zhang, K.; Tan, H.; Xu, Z.; Luan, F.; Guibas, L.; Wetzstein, G.; and Bi, S. 2025. Gaussian Mixture Flow Matching Models. *arXiv:2504.05304*.
- Chen, R. T. Q.; Rubanova, Y.; Bettencourt, J.; and Duvenaud, D. 2019. Neural Ordinary Differential Equations. *arXiv:1806.07366*.
- Chi, C.; Feng, S.; Du, Y.; Xu, Z.; Cousineau, E.; Burchfiel, B.; and Song, S. 2023. Diffusion Policy: Visuomotor Policy Learning via Action Diffusion. In *Proceedings of Robotics: Science and Systems (RSS)*.
- Cuturi, M. 2013. Sinkhorn Distances: Lightspeed Computation of Optimal Transportation Distances. *arXiv:1306.0895*.
- Guo, P.; and Schwing, A. G. 2025. Variational Rectified Flow Matching. *arXiv:2502.09616*.
- Gupta, A.; Kumar, V.; Lynch, C.; Levine, S.; and Hausman, K. 2019. Relay Policy Learning: Solving Long-Horizon Tasks via Imitation and Reinforcement Learning. *arXiv:1910.11956*.
- Handa, A.; Wyk, K. V.; Yang, W.; Liang, J.; Chao, Y.-W.; Wan, Q.; Birchfield, S.; Ratliff, N.; and Fox, D. 2019. DexPilot: Vision Based Teleoperation of Dexterous Robotic Hand-Arm System. *arXiv:1910.03135*.
- Hausman, K.; Chebotar, Y.; Schaal, S.; Sukhatme, G.; and Lim, J. 2017. Multi-Modal Imitation Learning from Unstructured Demonstrations using Generative Adversarial Nets. *arXiv:1705.10479*.
- Huang, C.-W.; Dinh, L.; and Courville, A. 2020. Augmented Normalizing Flows: Bridging the Gap Between Generative Flows and Latent Variable Models. *arXiv:2002.07101*.
- Jacobs, R. A.; Jordan, M. I.; Nowlan, S. J.; and Hinton, G. E. 1991. Adaptive Mixtures of Local Experts. *Neural Computation*, 3(1): 79–87.
- Jia, X.; Blessing, D.; Jiang, X.; Reuss, M.; Donat, A.; Lioutikov, R.; and Neumann, G. 2024. Towards Diverse Behaviors: A Benchmark for Imitation Learning with Human Demonstrations. *arXiv:2402.14606*.
- Jordan, M.; and Jacobs, R. 1993. Hierarchical mixtures of experts and the EM algorithm. In *Proceedings of 1993 International Conference on Neural Networks (IJCNN-93-Nagoya, Japan)*, volume 2, 1339–1344 vol.2.
- Kobyzev, I.; Prince, S. J.; and Brubaker, M. A. 2021. Normalizing Flows: An Introduction and Review of Current Methods. *IEEE Transactions on Pattern Analysis and Machine Intelligence*, 43(11): 3964–3979.
- Lipman, Y.; Chen, R. T. Q.; Ben-Hamu, H.; Nickel, M.; and Le, M. 2023. Flow Matching for Generative Modeling. *arXiv:2210.02747*.
- Liu, X.; Gong, C.; and Liu, Q. 2022. Flow Straight and Fast: Learning to Generate and Transfer Data with Rectified Flow. *arXiv:2209.03003*.
- Lu, G.; Gao, Z.; Chen, T.; Dai, W.; Wang, Z.; and Tang, Y. 2024. ManiCM: Real-time 3D Diffusion Policy via Consistency Model for Robotic Manipulation. *arXiv preprint arXiv:2406.01586*.
- Papamakarios, G.; Nalisnick, E.; Rezende, D. J.; Mohamed, S.; and Lakshminarayanan, B. 2021. Normalizing Flows for Probabilistic Modeling and Inference. *arXiv:1912.02762*.
- Peyré, G.; and Cuturi, M. 2020. Computational Optimal Transport. *arXiv:1803.00567*.
- Rajeswaran, A.; Kumar, V.; Gupta, A.; Vezzani, G.; Schulman, J.; Todorov, E.; and Levine, S. 2018. Learning Complex Dexterous Manipulation with Deep Reinforcement Learning and Demonstrations. *arXiv:1709.10087*.
- Rouxel, Q.; Ferrari, A.; Ivaldi, S.; and Mouret, J.-B. 2024. Flow Matching Imitation Learning for Multi-Support Manipulation. *arXiv:2407.12381*.
- Samaddar, A.; Sun, Y.; Nilsson, V.; and Madireddy, S. 2025. Efficient Flow Matching using Latent Variables. *arXiv:2505.04486*.
- Shridhar, M.; Manuelli, L.; and Fox, D. 2022. Perceiver-Actor: A Multi-Task Transformer for Robotic Manipulation. *arXiv:2209.05451*.
- Villani, C.; and Society, A. M. 2003. *Topics in Optimal Transportation*. Graduate studies in mathematics. American Mathematical Society. ISBN 9781470418045.
- Wang, C.; Fan, L.; Sun, J.; Zhang, R.; Fei-Fei, L.; Xu, D.; Zhu, Y.; and Anandkumar, A. 2023. MimicPlay: Long-Horizon Imitation Learning by Watching Human Play. *arXiv:2302.12422*.
- Wang, Y.; Zhang, Y.; Huo, M.; Tian, R.; Zhang, X.; Xie, Y.; Xu, C.; Ji, P.; Zhan, W.; Ding, M.; and Tomizuka, M. 2024a. Sparse Diffusion Policy: A Sparse, Reusable, and Flexible Policy for Robot Learning. *arXiv:2407.01531*.
- Wang, Z.; Li, Z.; Mandlkar, A.; Xu, Z.; Fan, J.; Narang, Y.; Fan, L.; Zhu, Y.; Balaji, Y.; Zhou, M.; Liu, M.-Y.; and Zeng, Y. 2024b. One-Step Diffusion Policy: Fast Visuomotor Policies via Diffusion Distillation. *arXiv:2410.21257*.
- Yang, L.; Zhang, Z.; Zhang, Z.; Liu, X.; Xu, M.; Zhang, W.; Meng, C.; Ermon, S.; and Cui, B. 2024. Consistency Flow Matching: Defining Straight Flows with Velocity Consistency. *arXiv:2407.02398*.
- Yu, T.; Quillen, D.; He, Z.; Julian, R.; Narayan, A.; Shively, H.; Bellathur, A.; Hausman, K.; Finn, C.; and Levine, S. 2021. Meta-World: A Benchmark and Evaluation for Multi-Task and Meta Reinforcement Learning. *arXiv:1910.10897*.
- Ze, Y.; Zhang, G.; Zhang, K.; Hu, C.; Wang, M.; and Xu, H. 2024. 3D Diffusion Policy: Generalizable Visuomotor Policy Learning via Simple 3D Representations. In *Proceedings of Robotics: Science and Systems (RSS)*.
- Zhang, F.; and Gienger, M. 2025. Affordance-based Robot Manipulation with Flow Matching. *arXiv:2409.01083*.
- Zhang, Q.; Liu, Z.; Fan, H.; Liu, G.; Zeng, B.; and Liu, S. 2024. FlowPolicy: Enabling Fast and Robust 3D Flow-based Policy via Consistency Flow Matching for Robot Manipulation. *arXiv:2412.04987*.

A Proofs

A.1 Notations of Ambiguity

Let $o \in \mathcal{O}$ be the observation, $t \in [0, 1]$ the (normalized) time, and $a \in \mathbb{R}^d$ the expert action. In the proof, we assume $\mathbb{E}\|a\|_2^2 < \infty$, which holds in real-world robot manipulation tasks.

Velocity-space setup (as in §4.1). Let $a_0, a_1 \in \mathbb{R}^d$ be two actions at the start and end of a flow path, and set

$$v^* = a_1 - a_0, \quad a_t = (1 - t)a_0 + ta_1, \quad t \in (0, 1).$$

A deterministic flow predictor $v_\theta(a_t, t, s)$ is trained with the mean-squared velocity loss

$$\mathcal{L}_{\text{vel}}(\theta) = \mathbb{E}[\|v^* - v_\theta(a_t, t, s)\|_2^2]. \quad (1)$$

The main text defines the corresponding *velocity ambiguity*

$$\mathcal{A}_{\text{FM}} = \mathbb{E}[\text{Var}[v^* \mid a_t, t, s]], \quad (2)$$

which lower-bounds any deterministic model’s loss.

This is the notation we used in the main text. However, this notation is indirectly linked to the action distribution in the dataset. For providing a more straightforward proof and intuition, below, we introduce an equivalent way to express ambiguity, based on action variance.

From velocity to action variance. Assume (i) the end-points a_0, a_1 are drawn *i.i.d.* from the same conditional distribution $p_\star(a \mid o, t)$ and (ii) the linear mixing rule above holds.

Applying the law of total variance yields

$$\mathcal{A}_{\text{FM}} = \frac{1}{t(1-t)} \mathbb{E}_{(o,t)}[\text{tr Var}(a \mid o, t)]. \quad (3)$$

Define

$$V_{\text{amb}} = \mathbb{E}_{(o,t)}[\text{tr } \Sigma_{o,t}], \quad \Sigma_{o,t} = \text{Var}[a \mid o, t]. \quad (4)$$

Equation (3) shows $\mathcal{A}_{\text{FM}} = \frac{1}{t(1-t)} V_{\text{amb}}$; both terms measure the same multimodal uncertainty, merely expressed in different coordinates. We therefore prove the lower bound in the simpler action space using V_{amb}

A.2 Irreducible Ambiguity of Deterministic Flow

Lemma A.1.1 For any deterministic flow f ,

$$\mathbb{E}[\|a - f(o, t)\|_2^2] = \underbrace{\mathbb{E}[\|a - \mu_{o,t}\|_2^2]}_{V_{\text{amb}}} + \mathbb{E}[\|\mu_{o,t} - f(o, t)\|_2^2].$$

$$\text{That is, } \mathcal{L}(f) = V_{\text{amb}} + \mathbb{E}[\|\mu_{o,t} - f(o, t)\|_2^2]. \quad (3)$$

Proof. Using $x = \mu_{o,t}$ and $y = f(o, t)$, expand

$$\|a - y\|^2 = \|a - x\|^2 + \|x - y\|^2 + 2(a - x)^\top (x - y).$$

Condition on (o, t) ; the mixed term vanishes because $\mathbb{E}[a - x \mid o, t] = 0$. Taking full expectation yields (3). \square

Theorem A.1.2 (Ambiguity lower bound).

$$\inf_f \mathcal{L}(f) = V_{\text{amb}}, \text{ achieved by } f^\star(o, t) = \mu_{o,t}. \quad (4)$$

Proof. Equation (3) implies $\mathcal{L}(f) \geq V_{\text{amb}}$ with equality iff the second term is zero, i.e. $f(o, t) = \mu_{o,t}$ almost surely. Hence the minimum attainable loss for deterministic flows is V_{amb} , reached by f^\star . \square

Proposition A.1.3 (Positive ambiguity at $t = 0$ under multi-modality). Fix an observation o and let the conditional action distribution at $t = 0$ be multi-modal, i.e. supported on at least two distinct actions $a^{(1)} \neq a^{(2)}$ with probabilities $\pi_1, \pi_2 > 0$. Then the conditional covariance satisfies $\text{tr } \Sigma_{o,t=0} > 0$, and consequently the task-level ambiguity $V_{\text{amb}}^{t=0} := \mathbb{E}_o[\text{tr } \Sigma_{o,0}]$ is strictly positive.

Proof. Consider the unit vector $u = (a^{(1)} - a^{(2)})/\|a^{(1)} - a^{(2)}\|$. The variance along u is

$$u^\top \Sigma_{o,0} u = \pi_1 [u^\top (a^{(1)} - \mu_{o,0})]^2 + \pi_2 [u^\top (a^{(2)} - \mu_{o,0})]^2 > 0,$$

so $\Sigma_{o,0}$ has a positive eigenvalue and non-zero trace. \square

Remark. The ambiguity term V_{amb} is fixed by the data’s conditional variance, providing a firm lower bound that no deterministic flow $f(o, t)$ can beat. When the expert distribution is multi-modal, the distinct modes necessarily “cross” at the initial time $t = 0$; this guarantees a non-degenerate conditional covariance $\Sigma_{o,0}$ and thus makes V_{amb} strictly positive.

A.3 Ambiguity Elimination by Latent

Theorem A.2. Assume that for every (o, t) the expert distribution can be written as a finite mixture

$$p_\star(a \mid o, t) = \sum_{k=1}^K \pi_k(o, t) \delta(a - a_k(o, t)), \quad \pi_k(o, t) > 0.$$

Introduce a discrete latent variable $z \in \{1, \dots, K\}$ with $q(z = k \mid o, t) = \pi_k(o, t)$ (i.e. exactly the mixture weights) and a latent-conditioned deterministic policy $f(o, t, z) = a_z(o, t)$. Then the expected mean-squared error satisfies

$$\mathbb{E}[\|a - f(o, t, z)\|_2^2] = 0.$$

Proof. Conditioned on $(o, t, z = k)$ the action a is deterministically $a_k(o, t)$, so $\|a - f(o, t, z)\|^2 = 0$ almost surely. Taking expectations over z and (o, t) preserves the zero value. \square

Remark. Theorem A.2 demonstrates an upper bound: with a perfectly aligned latent variable, the mean-squared risk can in principle be driven to zero. In practice one approximates the ideal latent assignment via a learned posterior or gating network, so residual error depends on the quality of that approximation. Introducing stochasticity or latent variables lets a policy match the *full* conditional distribution $p_\star(a \mid o, t)$ and thus circumvent this bound.

B Algorithms

B.1 Training Algorithm

Algorithm 1 describes the training procedure of our proposed VFP model.

Algorithm 1: VFP Training

```
1: Input: Demonstrations  $\mathcal{D} = \{(s_i, a_i)\}_{i=1}^N$ 
2: repeat
3:   Sample batched  $\{(s_i, a_i)\}_{i=1}^B$  from  $\mathcal{D}$ 
4:   Sample  $t \sim \mathcal{U}(0, 1)$  and  $a_0 \sim \mathcal{N}(0, I)$ 
5:   Compute  $a_t = ta_0 + (1 - t)a$ 
6:   Obtain  $z \sim q_\phi(z | s, a)$  using the encoder
7:   Compute MoE  $g(z)$  and  $v_{\theta, i}(a_t, t, s)$ 
8:   Compute the total loss  $\mathcal{L}_{\text{total}}$  in Eqn. (12)
9:   Update model parameters  $(\theta, \phi, \psi)$  by  $\nabla_{\theta, \phi, \psi} \mathcal{L}_{\text{total}}$ 
10: until converged
```

B.2 Inference Algorithm

Algorithm 2 presents the inference procedure.

Algorithm 2: VFP Sampling

```
1: while task not done do
2:   Observe current state  $s$ 
3:   Sample  $z \sim p_\psi(z | s)$ 
4:   Compute gating vector  $g(z)$  and select MoE expert(s)
5:   Sample  $a_0 \sim \mathcal{N}(0, I)$ 
6:   Integrate the ODE by Eqn. (1) using MoE decoder
    $da_t/dt = v_{\theta, i^*}(a_t, t, s)$ , with  $i^* = \arg \max_i g_i(z)$ 
7:   Execute action  $a$  in the robot environment
8: end while
```

C Experimental Details

Experimental protocols vary slightly across benchmarks, focusing primarily on performance and computational efficiency. For baselines with officially published results, we directly reference the performance reported in their original publications.

C.1 Evaluation Environments

All models are trained and evaluated on a single NVIDIA A5000 GPU across four benchmarks. For each method, we perform training runs using five distinct random seeds. The best-performing checkpoint from each seed, selected based on validation performance, is evaluated by conducting roll-outs over 30 episodes per seed. We report the mean and standard deviation of the performance metrics across these seeds. All inputs, including states and actions, are normalized to the interval $[-1, 1]$.

Notably, for measuring inference time, we perform experiments using a NVIDIA RTX 2080Ti GPU, same as our baseline FlowPolicy, providing a reliable basis for comparing efficiency across different methods.

D3IL. We select 3 tasks from D3IL (Jia et al. 2024), respectively Avoiding, Sorting-4, and Pushing. These tasks are all low-dimensional and rich of multi-modality, thus being a suitable environment for us to analyzing the multi-modal capabilities of methods. In these tasks, each model is trained for 2000 epochs, with evaluations conducted every 100 epochs.

Avoiding. The Avoiding task requires the robot to reach the green finish line from a fixed initial position without colliding with one of the six obstacles. The task does not require

object manipulation and is designed to test a model’s ability to capture diversity. There are 24 different ways of successfully completing the task. Thus, this task has very rich path multi-modality by design.

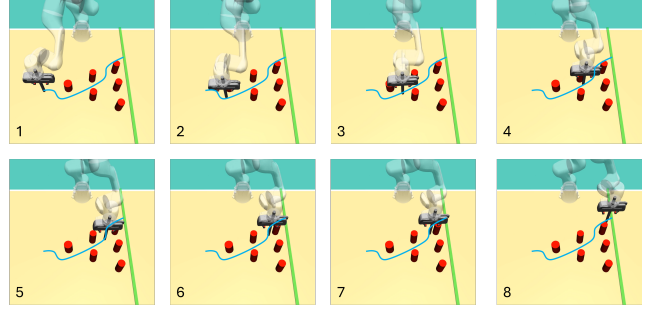


Figure 1: A single roll-out of VFP in Avoiding.

In this experiment, we utilize the officially provided dataset to train the models. The dataset contains 96 demonstrations in total, comprising 24 solutions with 4 trajectories for each solution. During training, we found that FlowPolicy converges fast compared to other method, as FlowPolicy simply converges to the average paths. In contrast, while VFP converges slower than FlowPolicy, our method can successfully capture the multi-modality.

Pushing. The task pushing requires the robot to push two blocks to fixed target zones. Conceptually, this task can be divided into two different tasks, pushing the red block and pushing the blue block. Therefore, it demands the model’s capability of capturing task multi-modality for completing this task.

Sorting-4. This task requires the robot to sort red and blue blocks to their color-matching target box. The ‘4’ here refers to the number of blocks. This task has many objects, is highly diverse, requires complex manipulations, has high variation in trajectory length, and is thus inherently very multi-modal.

Franka Kitchen. Franka Kitchen (Gupta et al. 2019) consists of a 9 DoF position-controlled Franka robot interacting with a kitchen scene that includes an openable microwave, four turnable oven burners, an oven light switch, a freely movable kettle, two hinged cabinets, and a sliding cabinet door. There are 7 valid tasks in the environment, and the robot is required to complete tasks in arbitrary order, as many as possible. Thus, we consider that this environment is a great instance of rich task multi-modality.

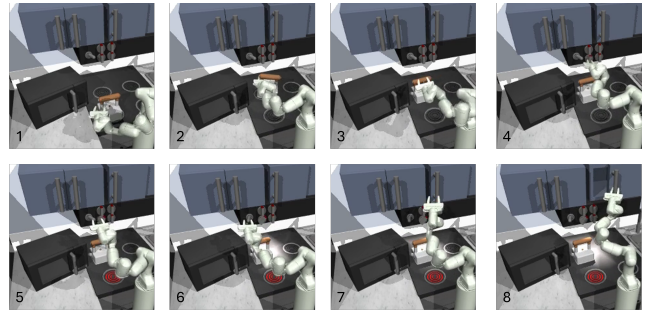


Figure 2: A single roll-out of VFP in Franka Kitchen.

We use the demonstrations dataset provided by Diffusion Policy (Chi et al. 2023). Each model is trained for 600 epochs and evaluated every 20 epochs.

Adroit. We evaluate on three Adroit (Rajeswaran et al. 2018) tasks—Hammer, Pen, and Door—each involving manipulation of a 24-DoF anthropomorphic Adroit hand (Fig. 3), which demands precise and coordinated control. This environment is particularly well-suited for assessing a policy’s ability to handle high-dimensional action space.

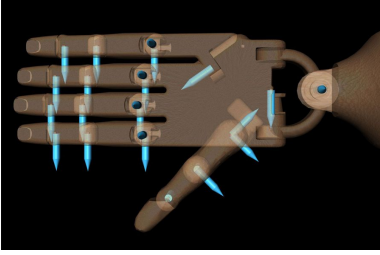


Figure 3: 24 degree of freedom ADROIT hand (Rajeswaran et al. 2018).

We generate 20 demonstration for each task by expert policies, provided by 3D Diffusion Policy (Ze et al. 2024). Each model is trained for 3000 epochs, with evaluations conducted every 200 epochs.

Meta-World. Meta-World (Yu et al. 2021) is a benchmark comprising 34 tasks of varying difficulty. Due to its large task set and diversity, it is particularly well-suited for evaluating a model’s general ability to learn a wide range of skills compared to earlier benchmarks. Demonstrations for these environments are generated by expert policies provided by 3D Diffusion Policy (Ze et al. 2024). Each model is trained for 3000 epochs, with evaluations conducted every 200 epochs.

D Implementation Details

The pipeline of Variational Flow Policy consists of a latent encoder, a prior network, and a Mixture-of-Experts (MoE) structured decode. For faster inference and a more compact model, the gating network in the MoE decoder can be removed, with its functionality integrated into the encoder and prior networks by setting the latent dimension equal to the number of experts. We now detail the implementations of each part as follows.

Latent Encoder. The latent encoder takes concatenated state-action pairs as input to predict the latent variable. In our implementation, we employ a multilayer perceptron (MLP) architecture consisting of shared hidden layers followed by two separate output layers for predicting the mean and variance, respectively. The flattened state and action vectors are concatenated before being fed into the network. We set `num_hidden_layers` to 3 and `hidden_dim` to 256. A simplified PyTorch implementation is given below:

```
1 class Encoder(nn.Module):
2     def __init__(
3         ...
```

```
4     ):
5         ...
6         layers = [nn.Linear(state_dim + action_dim,
7                             hidden_dim), activation()]
8         for _ in range(num_hidden_layers - 1):
9             layers.extend([
10                 nn.Linear(hidden_dim, hidden_dim),
11                 activation()])
12         self.shared_layers = nn.Sequential(*layers)
13         self.fc_mean = nn.Linear(hidden_dim,
14                                 latent_dim)
15         self.fc_logvar = nn.Linear(hidden_dim,
16                                 latent_dim)
17
18     ...
19     def forward(self, ...) -> torch.Tensor:
20         ...
21         x = torch.cat([state, action], dim=-1)
22         # Shared layers
23         h = self.shared_layers(x)
24         # Get distribution parameters
25         mean = self.fc_mean(h)
26         logvar = self.fc_logvar(h)
27         # Sample using reparameterization trick
28         z = self.reparameterize(mean, logvar)
29         return z
```

Latent Prior. The prior is implemented as a lightweight DDPM to ensure fast inference while producing multi-modality. Specifically, we use a compact denoising network and only a few diffusion steps. In our implementation, the denoising network is a small MLP with approximately 0.8×10^6 parameters in image/point-cloud-based settings (Adroit and Meta-World), and approximately 1.3×10^5 parameters in state-based settings (Franka Kitchen and D3IL). The number of denoising steps is set to 3.

Notably, in our design, the prior is not required to produce precise or high-fidelity latent values. Its role is solely to select a representative latent mode (i.e., to pick one expert from a mixture), rather than to reconstruct the exact posterior distribution. During inference, we apply a `top-k` operation with $k=1$ on the decoder’s gating logits, which effectively makes the system robust to inaccuracies in the prior output. This design allows the use of a minimal prior network without compromising performance, enabling fast and efficient inference.

Flow-based Experts. Our expert networks are largely based on the FlowPolicy architecture, where the core component is a `ConditionalUnet1D`. To improve efficiency, we reduce the model size by modifying only the down-sampling dimensions, while keeping the rest of the architecture unchanged. Specifically, we change the downsample dimensions from `[512, 1024, 2048]` to `[256, 1024, 2048]`, which significantly reduces computation without affecting performance.

For D3IL, where both the state and action dimensions are very low, we replace the U-Net with a MLP/Transformer as the backbone model.

Observation Encoder. For image/point-cloud-based environments such as Adroit and Meta-World, an observation encoder is required to process image or point-cloud inputs. In our implementation, we directly adopt the same encoder architecture as used in FlowPolicy, without modification.